Angewandte Chemie
International Edition

DOI: 10.1002/anie.201004718

**VIP Hydrogen Evolution**

# Low-Cost Hydrogen-Evolution Catalysts Based on Monolayer Platinum on Tungsten Monocarbide Substrates**

*Daniel V. Esposito, Sean T. Hunt, Alan L. Stottlemyer, Kevin D. Dobson, Brian E. McCandless, Robert W. Birkmire, and Jingguang G. Chen**

When powered by renewable energy sources, such as wind- or solar-based technologies, the generation of hydrogen from the electrolysis of water is a means to produce a high-energy-density, mobile energy carrier without any associated carbon dioxide emissions. At low temperatures, this process can take place in a variety of electrochemical devices, ranging from high-current-density polymer electrolyte membrane (PEM) electrolyzers to low-current-density, solar-driven photoelectrochemical cells (PECs). For all of these water-splitting applications, the choice of the hydrogen-evolution reaction (HER) catalyst employed at the cathode can have a profound influence on the cost, lifetime, and efficiency of the device. Platinum is a very active and commonly used HER catalyst, but its high price (US\$51.9 g$^{-1}$ as of March 2010)[1] and limited world-wide supply[2] make its use a barrier to mass production of $H_2$ by water electrolysis.

One approach to overcome the challenges associated with platinum HER catalysts is to increase the surface to bulk atomic ratio of platinum, thus allowing for a lower metal loading to be used without compromising electrolysis efficiency. Platinum electrocatalysts are typically in the form of supported nanoparticles, in which most platinum atoms are located within the particle core where they are screened from being involved in the electrochemical reaction. Herein, we explore the lower limit of platinum loading for the HER by utilizing nearly all platinum atoms in the form of an atomic layer, or monolayer (ML), on low-cost tungsten monocarbide (WC) substrates. For low-current-density applications, this ML catalyst may be deposited on a planar support, whilst for higher-current-density applications it should be incorporated on a high-surface-area mesoporous or particle-based support. In Figure 1, the potential to reduce platinum loading and its associated material cost at different HER current densities are estimated for ML Pt catalysts on planar, particulate, and mesoporous supports. When the ML Pt catalysts are compared to 5–10 nm Pt nanoparticles used in state-of-the-art PEM electrolyzers,[3] it is seen that an order of magnitude reduction in platinum loading may be achieved.

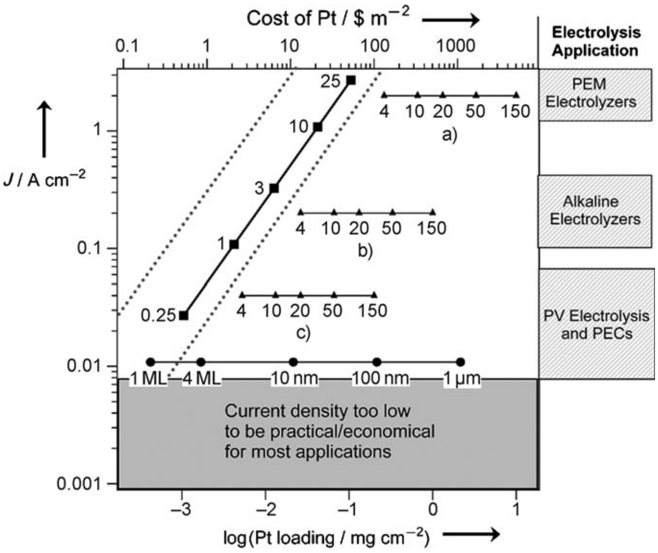

*Figure 1.* Relationship between platinum loading (lower axis) and cost (upper axis) and the HER current density *J* at constant overpotential $\eta = 80$ mV for various forms of platinum catalysts calculated using the Tafel equation: Spherical particles (▲; diameters in nm; a) 2 A cm$^{-2}$, b) 0.2 A cm$^{-2}$, c) 0.04 A cm$^{-2}$), thin films (●; thicknesses given), and mesoporous supported platinum (■; dotted lines signify variation in catalyst activity with the substrate material used; support surface areas in m$^2$ g$^{-1}$). Right side: ranges of operating current densities for various electrolysis devices. See the text and the Supporting Information for further details.

In Figure 1, it is assumed that ML Pt shows the same HER activity as bulk Pt, but for real catalysts, the properties of a ML of metal can be affected by its interactions with the substrate, leading to catalytic properties that are very different from the bulk metal.[4] These variations in catalytic activity result from perturbations to the electronic structure of the ML catalyst, which are attributed to two primary factors: deviation in interatomic distances caused by lattice strain, and the so-called ligand effect that arises from differences in the bimetallic bonds compared to those in bulk materials.[4]

A useful descriptor of these changes in electronic structure is the hydrogen binding energy (HBE), a parameter that correlates strongly with the HER activity, commonly expressed by its exchange current density $j_o$. Specifically, a plot of $\log(j_o)$ versus HBE produces a volcano-type curve that is characteristic of the Sabatier's principle whereby the best

---

[*] D. V. Esposito, S. T. Hunt, A. L. Stottlemyer, Prof. Dr. J. G. Chen
Center for Catalytic Science and Technology
University of Delaware, Newark, DE 19716 (USA)
Fax: (+1) 302-831-2085
E-mail: jgchen@udel.edu
D. V. Esposito, Dr. K. D. Dobson, B. E. McCandless,
Prof. Dr. R. W. Birkmire
Institute of Energy Conversion
University of Delaware, Newark, DE 19716 (USA)

[**] We acknowledge financial support from the U.S. Department of Energy (Grant No. DE-FG02-00ER15104).

Supporting information for this article is available on the WWW under http://dx.doi.org/10.1002/anie.201004718.

catalysts for a given system are those that exhibit intermediate binding energies for reactive intermediates.[5] In recent years, experimental and theoretical studies of ML Pd catalysts, selected based on HBE values located at the center of the volcano curve, showed the potential of ML bimetallic surfaces to achieve HER exchange current densities that exceed Pt.[6] However, the utility of these catalysts is limited by the high costs of the precious metal substrates used in that study. A density functional theory (DFT)-based combinatorial screening analysis of over 700 ML bimetallic surfaces was conducted in an attempt to find other active HER catalysts,[7] but none of those identified were predicted to have HER activity and electrochemical stability equal or greater than platinum.

Herein, we provide theoretical and experimental evidence that low-cost WC can be used as a substrate for ML Pt, resulting in a catalyst with very high HER activity. WC is known for its "platinum-like" catalytic properties[8] and exhibits good stability in acidic environments over a wide potential range.[9,10,11] WC catalysts have also shown great promise as support materials for platinum particles,[12] leading to improved catalyst stability[13] and synergistic activity in a variety of electrochemical systems.[14] The common catalytic properties and good adhesion of Pt on WC are attributed to similarities in the electronic structures of the two materials.[12] Given these similarities, it is expected that the bimetallic ligand effect for ML Pt-WC should be small, resulting in a surface whose electronic and chemical properties should not deviate substantially from that of bulk Pt.

To test this hypothesis, DFT was used to calculate the HBE of closed-packed surfaces of Pt(111), WC(0001), and ML Pt-WC(0001). In Table 1, the results of these calculations are shown for a hydrogen coverage of 1/9 ML. The HBE for the unmodified WC surface is significantly greater than Pt, but that of 1 ML of Pt on WC is almost identical to that of bulk Pt, suggesting the possibility of maintaining a catalytically active platinum surface while replacing its bulk with " platinum-like" WC. This argument is supported by the comparison of the surface d-band density of states (DOS) of the three surfaces (see the Supporting Information). The d-band DOS of WC(0001) is characterized by many states near or above the Fermi level. In contrast, the surface d-band DOS is shifted to below the Fermi level upon the deposition of ML Pt, making the electronic properties of ML Pt-WC(0001) very similar to that of Pt(111). According to previous studies,[4,15] the surface d-band position is related to the values of HBE, with the binding energy decreasing as the d-band center shifts away from the Fermi level. Therefore the comparison of the d-band DOS of the three surfaces are consistent with the HBE values in Table 1.

***Table 1:*** DFT-calculated per-atom hydrogen binding energies (HBE) for WC, Pt, and 1 ML Pt-WC surfaces with a hydrogen coverage of 1/9 ML.[a]

| Surface | HBE [eV] |
|---|---|
| WC(0001) | −0.99 |
| Pt(111) | −0.46 |
| 1 ML Pt-WC(0001) | −0.43 |

[a] See the Experimental Section for more details on HBE calculations.

To verify the DFT prediction that 1 ML Pt-WC should display HER activity similar to platinum, we have deposited sub-ML to ML coverages of Pt on smooth, single-phase WC thin films. For comparison, a polycrystalline platinum foil and a "thick platinum" sample consisting of 30 equivalent Pt MLs on WC were also studied. WC thin films were deposited on polycrystalline tungsten foils by reactive magnetron sputtering using a WC target. Platinum was then deposited on these WC thin films by thermal evaporation, a process that has been shown to proceed by a layer-by-layer growth mechanism for the first two ML on polycrystalline WC foil.[16] In Figure 2a, glancing incidence X-ray diffraction (GIXRD) patterns are shown for WC and 30 ML Pt-WC taken at an incident angle of 1°, representing a sampling depth of about 70 nm in pure WC.[17] The pattern for the unmodified WC substrate is seen to be single-phase WC,[17] with no impurity phases present. Relatively weak Pt(111) and Pt(110) peaks are observed only at very high platinum loadings, as shown for the 30 ML Pt-WC thin film in Figure 2a. Analysis of X-ray photoelectron spectroscopy (XPS) scans for the as-synthesized surfaces reveals atomic ratios of tungsten to carbidic carbon of approximately 1:1, which is consistent with GIXRD results. In Figure 2b, the low binding energy region of XPS scans for Pt, WC, and several Pt-WC films are compared. From the peak areas of the Pt 4f and W 4f XPS peaks, the equivalent ML of deposited Pt were calculated as described in the Supporting Information.

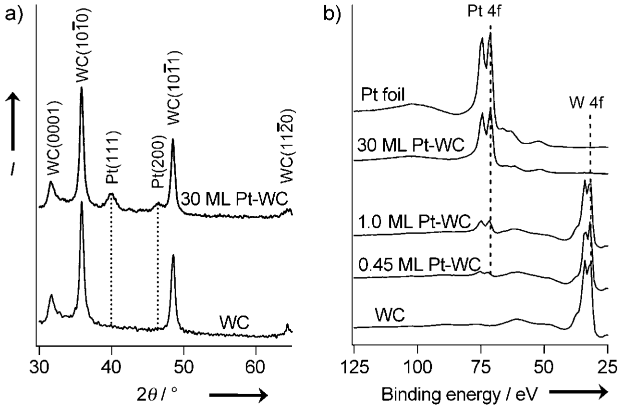

***Figure 2.*** a) Glancing-incidence XRD patterns for the as-synthesized WC and 30 ML Pt-WC thin film electrodes. b) Low-binding-energy region of XPS scans for WC, Pt, and Pt-WC thin films. (See the Supporting Information for more detailed characterization of the ML Pt-WC surfaces.)

The HER activity of the Pt-modified WC surfaces was tested in 0.5 M $H_2SO_4$ at room temperature. In Figure 3, the HER overpotentials ($\eta$) for WC, Pt, and several Pt-WC surfaces are shown as a function of the logarithm of the current density to give a plot known as a Tafel curve that is commonly used for analysis of the HER and other electrochemical reactions. Qualitatively, it is seen that the activity of unmodified WC is significantly lower than the bulk platinum

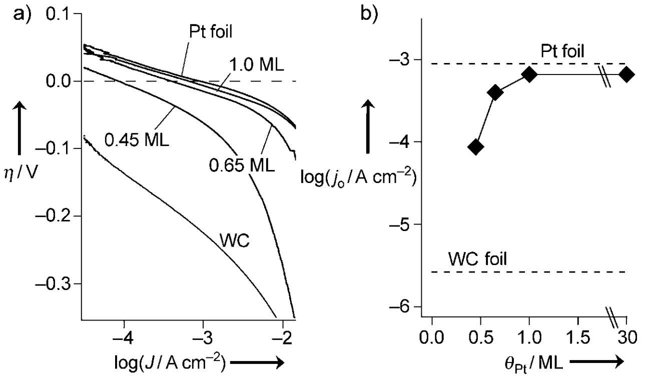

**Figure 3.** a) Tafel plots for WC, Pt, and sub-ML to ML Pt-WC foils in 0.5 M $H_2SO_4$. Measurements were taken with a scan rate of 2 mV s$^{-1}$. b) Dependence of the HER exchange current density ($j_o$) on the equivalent coverage of Pt deposited ($\theta_{Pt}$).

foil. However, the activity of WC is substantially enhanced upon the addition of sub-ML amounts of platinum, and the activity of 1 ML of Pt on WC gives a Tafel plot that is almost identical to that of the platinum foil. The $j_o$ values for WC and platinum foil surfaces are in agreement with those reported in literature for smooth, polycrystalline Pt[18] and WC[19] surfaces under similar conditions. In Figure 3 b, a plot of log($j_o$) versus platinum coverage on WC shows that the HER activity of the Pt-WC surface approaches that of bulk platinum foil at around a Pt coverage of 1 ML. The slight difference in $j_o$ values between the 30 ML Pt-WC and platinum foil samples could arise from differences in crystal orientation or true surface area. The similar HER activity of 1 ML Pt-WC to bulk Pt is consistent with our DFT predictions based on the well-established correlation between $j_o$ and HBE values.[18]

For ML electrocatalysts, electrochemical stability becomes especially crucial to device operation as the loss of the top ML will result in complete change in the electrocatalytic activity. To test the short-term stability of the ML Pt-WC samples studied in this work, the atomic ratio of Pt to W, calculated from the areas of the Pt 4f and W 4f XPS peaks, was compared before and after HER measurements (Figure 4). All of the samples retained a near-constant atomic ratio before and after electrochemical tests, indicating that the Pt-WC surface maintained its ML structure over short times in the HER environment in $H_2SO_4$. If any of the platinum overlayer were dissolved into solution, or if ML Pt were to agglomerate to form platinum particles on the WC surface, the atomic Pt/W ratio would undergo a notable reduction. Further discussion on the stability of the ML Pt-WC catalysts can be found in the Supporting Information.

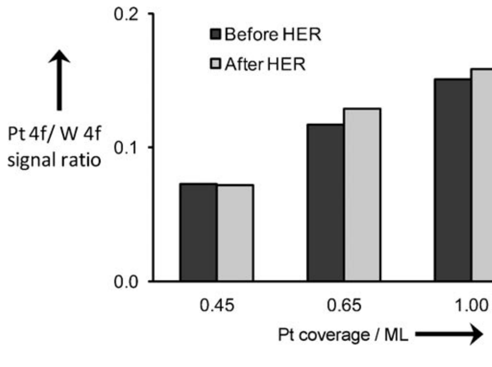

**Figure 4.** XPS Pt 4f/W 4f intensity ratios for Pt-WC samples before and after electrochemical HER measurements in 0.5 M $H_2SO_4$.

Although planar WC foil substrates were used in this work, a substrate material for ML catalysts can take many different forms dependant on the application. Low-surface-area supports may be used in low-current-density applications, such as PEC and PV electrolysis, whereas high-current-density applications will require mesoporous or particulate supports. In the latter case, a commonly considered catalyst structure is a core–shell nanoparticle, for which the ML catalyst forms a shell layer around the particle core. Similarly, a mesoporous support could be coated by the ML catalyst. For these high-surface-area ML catalysts, the shell component could be created by various synthesis techniques, such as atomic layer deposition, reverse micelles for deposition on particles, or electrodeposition. Development of these high-surface-area Pt-WC core–shell materials will be critical for the use of ML Pt-WC HER catalysts in the high current density applications shown in Figure 1.

In summary, we have shown that 1 ML Pt-WC films can be used as HER catalysts that show activity comparable to that of bulk platinum. Our combined experimental and theoretical results provide important insights into the understanding of the so-called platinum-like properties of WC. Based on the DFT calculations of HBE and the experimentally measured HER activity, the surface electronic and chemical properties of WC are not exactly platinum-like. However, the bulk properties of WC are very intriguing, and WC appears to be an ideal substrate to support platinum. The surface electronic and chemical properties of ML Pt on the bulk WC substrate are very similar to those of bulk platinum, thus demonstrating the possibility that all but the topmost layer of platinum can be replaced by WC. In this regard, ML Pt-WC is very platinum-like. These ML Pt-WC catalysts represent a significant decrease in platinum loading and associated platinum cost compared to that currently used in many electrolysis applications. Further work is needed to develop high-surface-area ML Pt-WC structures for high-current-density applications and to investigate the long-term stability of this type of promising HER catalyst. Finally, considering the electrochemical stability of WC, the ML Pt-WC systems should be promising materials to replace bulk platinum in other electrochemical and photoelectrochemical applications.

## Experimental Section

Platinum foil (Alfa Aesar, 99.99% pure) was used as received. WC thin films were deposited on polycrystalline tungsten foil (Alfa Aesar, 99.99% pure) by physical vapor deposition through magnetron sputtering using a WC target in a vacuum chamber with a base pressure of $5\times10^{-8}$ Torr. Deposition was conducted in an argon-, dihydrogen-, and ethylene-containing environment, followed by a high temperature post annealing to 1273 K in flowing $H_2$ and $CH_4$ inside a quartz tube furnace. Platinum was deposited on WC thin films by the thermal evaporation from a platinum wire wrapped around a resistively heated tungsten filament. The coverage of platinum deposited on the WC substrates was determined from XPS measurements as described in the Supporting Information. For each sample, the homogeneity of the platinum overlayer was verified by checking the Pt 4f/W 4f signal ratio in 2–3 locations.

The HER activity of various foil electrodes was tested in argon-purged 0.5 M $H_2SO_4$ at room temperature using a standard three-electrode set-up employing a Princeton Applied Research PARSTAT 2273 potentiostat. To condition the electrodes, 25 CV cycles were conducted between 0.0 V (vs. the normal hydrogen electrode, NHE) and the onset of oxidation at $50\,\mathrm{mV\,s^{-1}}$. Tafel curves were then obtained from linear sweep voltammograms using a scan rate of $2\,\mathrm{mV\,s^{-1}}$. Homogeneity of the platinum-modified surfaces was confirmed by the observation of uniform $H_2$ gas evolution from the electrode surfaces.

Hydrogen binding energies were calculated using density functional theory (DFT) with the PW91 functional and the Vienna ab initio Simulation Package (VASP). Each calculation used $3 \times 3$ surface cells. The WC surfaces contained six layers of atoms and twelve layers of vacuum, whilst the Pt(111) surface contained four layers of atoms and ten layers of vacuum. The bottom layers were fixed whilst the top two layers were allowed to relax. For all surfaces, a $3 \times 3 \times 1$ Monkhorst–Pack automatic k-point mesh and a plane wave cutoff of 396 eV was used. DFT results were used to calculate the HBE as defined by Nørskov et al.[18]

Received: July 30, 2010

**Keywords:** electrocatalysis · hydrogen evolution reaction · monolayers · platinum · tungsten carbide

---

[1] Johnson Matthey Plc, “Platinum Prices” can be found under http://www.platinum.matthey.com/pgm-prices/price-charts/.

[2] C. J. Yang, *Energy Policy* **2009**, *37*, 1805.

[3] S. A. Grigoriev, P. Millet, V. N. Fateev, *J. Power Sources* **2008**, *177*, 281.

[4] J. G. Chen, C. A. Menning, M. B. Zellner, *Surf. Sci. Rep.* **2008**, *63*, 201.

[5] P. Sabatier, *Catalysis in Organic Chemistry*, D. Van Nostrand Company, New York, **1922**.

[6] J. Greeley, J. K. Norskov, L. A. Kibler, A. M. El-Aziz, D. M. Kolb, *ChemPhysChem* **2006**, *7*, 1032.

[7] J. Greeley, T. F. Jaramillo, J. Bonde, I. B. Chorkendorff, J. K. Norskov, *Nat. Mater.* **2006**, *5*, 909.

[8] H. H. Hwu, J. G. Chen, *Chem. Rev.* **2005**, *105*, 185.

[9] B. Bozzini, G. P. De Gaudenzi, A. Fanigliulo, C. Mele, *Corros. Sci.* **2004**, *46*, 453.

[10] E. C. Weigert, D. V. Esposito, J. G. Chen, *J. Power Sources* **2009**, *193*, 501.

[11] E. C. Weigert, A. L. Stottlemyer, M. B. Zellner, J. G. Chen, *J. Phys. Chem. C* **2007**, *111*, 14617.

[12] Y. Y. Shao, J. Liu, Y. Wang, Y. H. Lin, *J. Mater. Chem.* **2009**, *19*, 46.

[13] H. Chhina, S. Campbell, O. Kesler, *J. Power Sources* **2007**, *164*, 431.

[14] M. K. Jeon, K. R. Lee, W. S. Lee, H. Daimon, A. Nakahara, S. I. Woo, *J. Power Sources* **2008**, *185*, 927.

[15] J. R. Kitchin, J. K. Norskov, M. A. Barteau, J. G. Chen, *Catal. Today* **2005**, *105*, 66.

[16] M. P. Humbert, C. A. Menning, J. G. Chen, *J. Catal.* **2010**, *271*, 132.

[17] D. V. Esposito, K. D. Dobson, B. E. McCandless, R. W. Birkmire, J. G. Chen, *J. Electrochem. Soc.* **2009**, *156*, B962.

[18] J. K. Nørskov, T. Bligaard, A. Logadottir, J. R. Kitchin, J. G. Chen, S. Pandelov, U. Stimming, *J. Electrochem. Soc.* **2005**, *152*, J23.

[19] G. A. Tsirlina, O. A. Petrii, *Sov. Electrochem.* **1985**, *21*, 65.